JOURNAL OF AIRCRAFT
Vol. 39, No. 1, January–February 2002

Predicting the Dynamic Behavior of a Coupled Structure Using Frequency-Response Functions

T. P. Gialamas,* D. A. Manolas,* D. T. Tsahalis†
University of Patras, 26500 Patras, Greece

The mathematical formulation of the coupling method that allows the prediction of the dynamic behavior of a coupled structure by means of frequency-response functions (FRFs) of the components it consists of is well established. However, this method fails to perform in many cases. The main deficiencies are the omission of the rotational degrees of freedom, due to the difficulty in measuring FRFs for these degree of freedom, and the direct inversion of the summation matrix of the component FRFs at the coupling points, the core of the coupling method. During the investigation of these deficiencies, it was found that the lack of information about the rotational degrees of freedom lead to a negative frequency shift of the predictions. It was also proven, by means of singular value decomposition (SVD) theory, that the difficulties encountered during the direct inversion of the matrix are due to ill-conditioning effects. Additionally, a pseudoinversion was applied utilizing the SVD theory, which led to an improvement in the accuracy of the coupling procedure for the majority of the cases. Finally, for the instances where inaccuracies persisted, a new algorithm was developed and shown to improve the pseudoinversion results greatly.

Nomenclature

$[G]$	=	$(n \times m)$ complex matrix
$[H]$	=	frequency-response function (FRF) matrix
$\lfloor H \rfloor$	=	row of FRF's matrix
$\{H\}$	=	column of FRF's matrix
i, j	=	degrees of freedom (DOF) out of the interface
r, m	=	indices
S	=	DOF on the interface
$[U]$	=	$(n \times n)$ unitary matrix, that is, $[U][U]^H = [U]^H[U] = [I]$; columns called left singulars vectors
$[V]$	=	$(m \times m)$ unitary matrix; columns called right singulars vectors
$[\Sigma]$	=	$(n \times m)$ real, pseudodiagonal matrix; elements called singular values and assumed, without loss of generality, to be arranged in decreasing order
σ	=	singular value

I. Introduction

IF the prediction of the dynamic behavior of a coupled structure is required, either the analytical and/or the numerical approach can be used.[1,2] However, practice has shown that these methods exhibit significant deficiencies. Indeed, it is rather difficult to model a structure that comprises many parts as one entity. Furthermore, in the majority of the cases, the irregularities that are present in any real structure cannot be included in an analytical/numerical model. The same goes for the damping because its accurate description is rarely possible. An alternative approach, which overcomes these two particular drawbacks, is the experimental one, which makes use of the measurements of the coupled structure. In this case, there is no concern about the characteristic features, that is, local irregularities, or damping of the structure because these are inherently present in the measurements. However, experience has shown that it is difficult to perform measurements on the total structure itself because its size and/or complexity may give rise to many problems in the application of the excitation, as well as in the acquisition of the responses. Furthermore, when a modification of the total structure is required, the whole set of the measurements must be performed on the modified coupled structure.

An alternate approach is provided through the coupling technique, which is described in detail in the next section. This method overcomes the majority of the described problems because it makes direct use of the measured frequency-response functions (FRFs) of the individual substructures of the coupled structure. However, despite the promising features of this method and its mathematical formulation being well established, it is common for the coupling predictions to fail to give acceptable results. There are two main reasons for this failure.

The first reason stems from the fact that very often the formulation of the full FRF matrices of the substructures is practically impossible, due to the difficulty of obtaining excitation and response measurements of the rotational degrees of freedom (RDOF). Consequently, these DOF are neglected during the analysis. However, as it has been reported by many researchers in the past, the lack of the RDOF is a major obstacle to the correct prediction of the response.[3–5]

The second reason is attributed to the direct inversion of the summation matrix of the substructures FRFs at the coupling points, as is dictated by the mathematical formulation.[6] Indeed, because the matrix to be inverted is based on measurements, it suffers from ill-conditioning effects. Thus, as has already been reported,[7–9] significant problems are encountered during the calculation of the inverse matrix. This paper deals with these two major source of erroneous results. Specifically, it reveals what effect the lack of information about RDOF has on the predictions. Furthermore, it presents a technique of inversion along with a new improvement algorithm, which decreases significantly the negative influence of the ill-conditioning effects. The paper is organized as follows. First, the mathematical formulation of the coupling method that employes measured FRFs is given. Second, the experimental procedure is described. Third, the effect of the RDOF is revealed by means of finite element simulations. A physical interpretation of the conclusions reached is given by means of the modes of the structure under examination. Fourth, the singular value decomposition (SVD) theory is employed to present 1) a procedure by which the condition of the matrix to be inverted can be assessed before the direct inversion takes place and 2) an inversion technique (pseudoinversion) that improves the results of the coupling procedure by reducing the negative effects

Received 7 November 2000; revision received 24 May 2001; accepted for publication 26 May 2001.

*Ph.D. Student, Laboratory of Fluid Mechanics and Energy, Chemical Engineering Department, P.O. Box 1400.

†Professor, Laboratory of Fluid Mechanics and Energy, Chemical Engineering Department, P.O. Box 1400.

of the direct inversion. Finally, a new algorithm is presented that improves further the pseudoiversion results.

II. Basic Theory

Consider two substructures A and B that are coupled together at s interconnection points to form a new structure C. Then if the equation of motion for the two substructures and the equilibrium conditions for the forces, as well as the compatibility conditions for the displacements at the points that belong to the coupling interface, are taken into account, the dynamic behavior of structure C can be obtained by means of the following equations.[6]

If both DOF i and j are on substructure A,

$$H_{C_{ij}} = H_{A_{ij}} - \lfloor H_A \rfloor_{iS} \left([H_A]_{SS} + [H_B]_{SS} \right)^{-1} \{H_A\}_{Sj} \qquad (1)$$

If both DOF i and j are on substructure B,

$$H_{C_{ij}} = H_{B_{ij}} - \lfloor H_B \rfloor_{iS} \left([H_A]_{SS} + [H_B]_{SS} \right)^{-1} \{H_B\}_{Sj} \qquad (2)$$

If DOF i is on substructure A and DOF j is on the substructure B,

$$H_{C_{ij}} = \lfloor H_A \rfloor_{iS} \left([H_A]_{SS} + [H_B]_{SS} \right)^{-1} \{H_B\}_{Sj} \qquad (3)$$

Finally, if DOF i is on the substructure B and DOF j is on the substructure A,

$$H_{C_{ij}} = \lfloor H_B \rfloor_{iS} \left([H_A]_{SS} + [H_B]_{SS} \right)^{-1} \{H_A\}_{Sj} \qquad (4)$$

Each of the these formulations is valid at the coupling points. In the present study, investigations concerning only the coupling points are carried out, and Eq. (3) is employed for the predictions of the dynamic behavior of the coupled structure.

III. Experimental Procedure

A. Test Structure

The test structure for which the measurements and the simulations were performed is shown in Fig. 1. The connection between the two substructures was feasible through three foreseen connecting flaps. A very strong structural glue was used, to achieve a coupling as rigid as possible. To achieve free–free boundary conditions, the structures were suspended by soft shockcords.

B. Measurements

The FRFs at the points that belong to the coupling interface were measured for both the substructures and the coupled structure. The latter set of measurements is used as a basis of comparison with the results that are derived from the prediction formulas. The excitation of the structures was created by a roving hammer. As far as the direction of the measurements is concerned, only the vibration pattern orthogonal to the vibrating plane was measured for each point because the vibrations in the other directions were negligible. A complete description of the experimental procedure is available.[10]

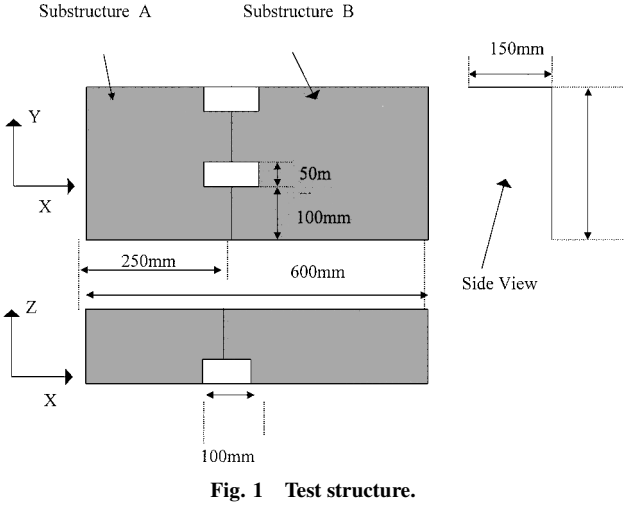

Fig. 1 Test structure.

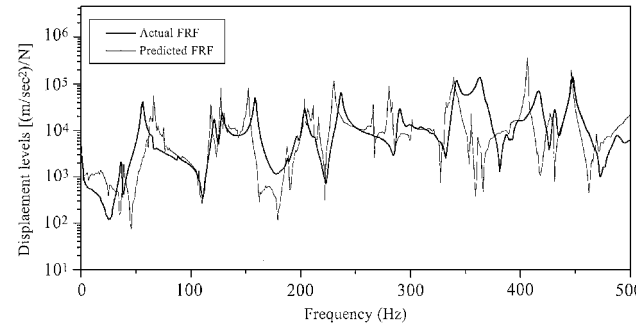

Fig. 2 Comparison between actual ad predicted FRF.

IV. Investigation of the Effect of the RDOF

In Fig. 2, a comparison between a directly measured FRF of the coupled structure and the prediction of the same FRF [which was calculated by means of Eq. (3)] is presented. Generally speaking, the synthesized FRF predicts the measured results quite well. However, two significant problems can be identified: 1) A negative frequency shift of the peaks is exhibited by the predicted FRF. 2) In some frequency bands, the predicted FRF is not smooth (especially in the lower frequencies) and presents some false peaks. This section deals with the former issue.

To investigate whether the lack of the RDOF was responsible for this negative frequency shift, finite element (FE) simulations were carried out. Subsequently, the coupling technique was applied, using the data obtained from the finite element analysis. Note that, as far as the translational DOF (TDOF) are concerned, only the ones that were measured during the experimental procedure were taken into account in the FE analysis.

In Fig. 3, two plots are given using numerically (FE analysis) calculated FRFs for the two substructures and for the coupled structure. From Fig. 3a, where only the TDOF are taken into account, a behavior similar to the one that was observed when experimental data were used can be seen. However, when the RDOF are included in the calculations, there is a better match between the predicted FRFs (using the numerically calculated FRFs of the two substructures) and the numerically calculated ones for the coupled structure (Fig. 3b). However, two new inaccuracies are observed.

First, some new peaks appear at the lower frequencies. Close investigation reveals that the appearance of the majority of the new peaks can be attributed to the additional rotational information that is introduced in the predictions.

Second, some peaks are not as well predicted when RDOF are included in the predictions. An interpretation is sought through the extraction of the modes of the coupled structure and the substructures. Particularly, two representative cases are chosen to be investigated. In the first case, better prediction of a peak is achieved, whereas in the second case, the prediction of a peak is worse when the RDOF are included. As an example of the first case, the peak that exists at the 171.91 Hz is examined.

When the modes of the two substructures are examined, a mode of substructure A at 166.73 Hz and one at 176.58 Hz for the substructure B can be found. This is expected because if two modes, each from different substructure, are coupled, then the mode of the coupled structure must be located in a natural frequency somewhere between the natural frequencies of the two substructures. When the modes of the two substructures and of the coupled structure are observed, it becomes apparent from the motion of the coupling points that these are in phase.[11] In Ref. 11 it can be seen that the modes are neither pure translational nor pure rotational. Specifically, a tendency of the two substructures to rotate around Y and Z axes can be identified. This tendency supports that there is an improvement to the predictions when RDOF are used.

As an example of the second case, a peak that is placed at 235.73 Hz is investigated. Obviously, the prediction of this peak is worse when RDOF are included (Fig. 3). A detailed study proves that the RDOF that causes the movement of the predicted peak from 235 to 250 Hz is the rotation around the Y axis.[11] Based on this,

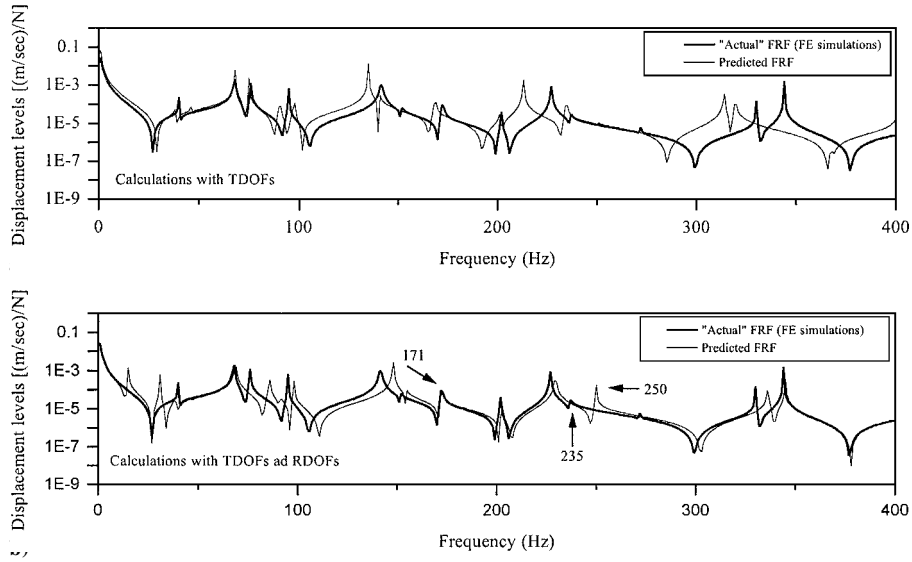

Fig. 3 Comparison between actual and predicted FRF (FE simulations are used).

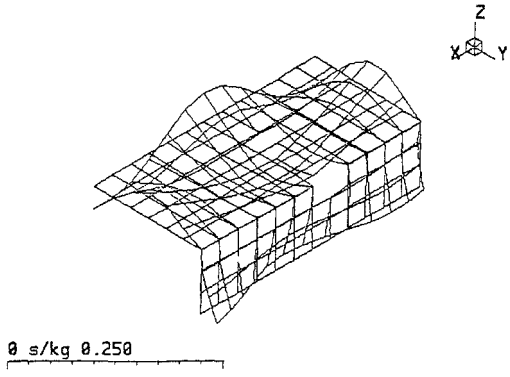

Fig. 4 Mode of the coupled structure at 235.73 Hz.

the following explanation can be given: When it is taken into consideration that, when the two substructures are coupled, the rotation around the Y axis is eliminated for the points that belong at the coupling interface, as well as that the mode of the coupled structure at 235.73 Hz is a pure translational one (Fig. 4), then it can be claimed that by inserting the rotation around Y the results are distorted.

V. Pseudoinversion by SVD

To determine if the inversion of the matrix that is required by the coupling technique [Eqs. (1–4)], called $[SS]$ from now on because it refers to the coupling points, causes the problem of the extra peaks, as well as of the rough results, the SVD theory is adopted. According to this theory, a $(n \times m)$ complex matrix $[G]$ can be decomposed as follows:

$$[G] = [U][\Sigma][V]^H \tag{5}$$

One of the most useful applications of the SVD is the condition number, which is defined as the ratio of the largest singular value to the minimum one. If this number is large, then the matrix is ill conditioned and problems will be encountered during its direct inversion. From Fig. 5, where five out of nine singular values of $[SS]$ are plotted, it can be deduced that the condition number (σ_1/σ_9) is large for the majority of the frequencies. Therefore, the additional false peaks, as well as the appearance of rough results at the lower frequencies, can be attributed to the direct inversion of $[SS]$. Thus, it is of major importance to define an alternative form of inversion that will overcome these problems. Such an inversion is the pseudoinversion, by means of SVD, which is proposed in this study as

$$[A]^+ = [V]_r[\Sigma]_r^{-1}[U]_r^H \tag{6}$$

The index r indicates that at each frequency line only the r $(r < m)$ larger nonzero singular values are used. The others are set equal to zero. For the specific case under examination, all of the singular values that were larger than 1% of the largest singular value, tolerance 1% (TOL 1%), were taken into account in each frequency line. The results obtained by the application of Eq. (3) using pseudoinversion instead of direct inversion, are plotted in middle part of Fig. 6. Generally speaking, it can be claimed that the ill-conditioned effects have been smoothed out, leading to better predictions than that achieved when the direct inversion is applied (top Fig. 6). However, new difficulties seem to arise when the pseudoinversion is employed. Particularly, there is a chopping of some peaks, and in some cases, new, well-separated peaks are noticed. To justify this behavior the following arguments are offered.

Consider the SVD of matrix $[SS]$:

$$[SS] = \left([H_A]_{SS} + [H_B]_{SS}\right) = [U][\Sigma][V]^H \tag{7}$$

The ith singular value of the summed matrix can be considered as the summation of the contributions of the two components,

$$\sigma_1 = \sigma_{Ai} + \sigma_{Bi} \tag{8}$$

From the combination of Eqs. (7) and (8), the following equation can be obtained:

$$\sigma_i = \{U_i\}^H[H_A]_{SS}\{V_i\} + \{U_i\}^H[H_B]_{SS}\{V_i\} \tag{9}$$

From Eq. (9) it is obvious that small singular values of matrix $[SS]$ at a frequency line can be due to small contributions or from large but opposite contributions from the components. In the latter case, the elimination of the singular values during the pseudoinverion leads to loss of valuable structural information.

To test this argument, two representative cases were chosen and examined in detail: the frequency range 279–282 Hz (chopping of the peak) and the frequency range 404–407 Hz (appearance of two, well separated peaks instead of one) (middle Fig. 6).

A. Frequency Range 404–407 Hertz

As presented previously,[12] the number of the singular values that should be taken into account during the pseudoinversion can be estimated by the rank of the matrix. Calculating the rank of $[SS]$ (using TOL 1% as for the case of the pseudoinversion), it is determined that in this range only the last singular value is neglected. When the real parts of the contributions of the two substructures to the last singular value are examined, it can be seen that these are large

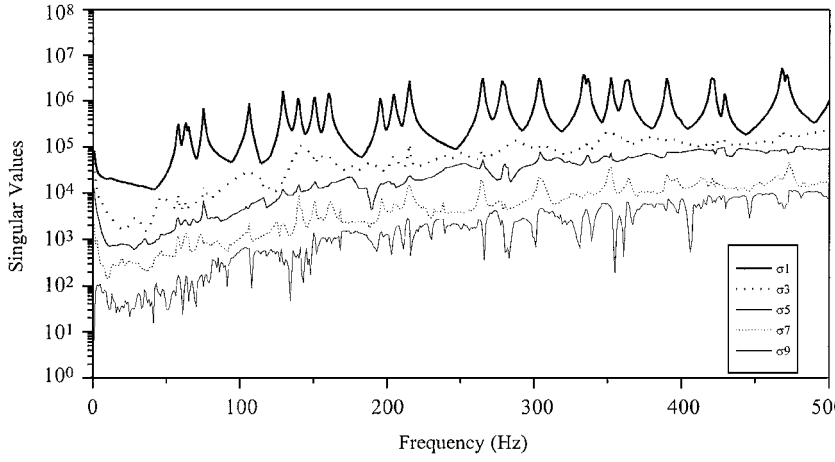

Fig. 5 Singular values of [*SS*]: $\sigma 1 > \sigma 3 > \sigma 5 > \sigma 7 > \sigma 9$.

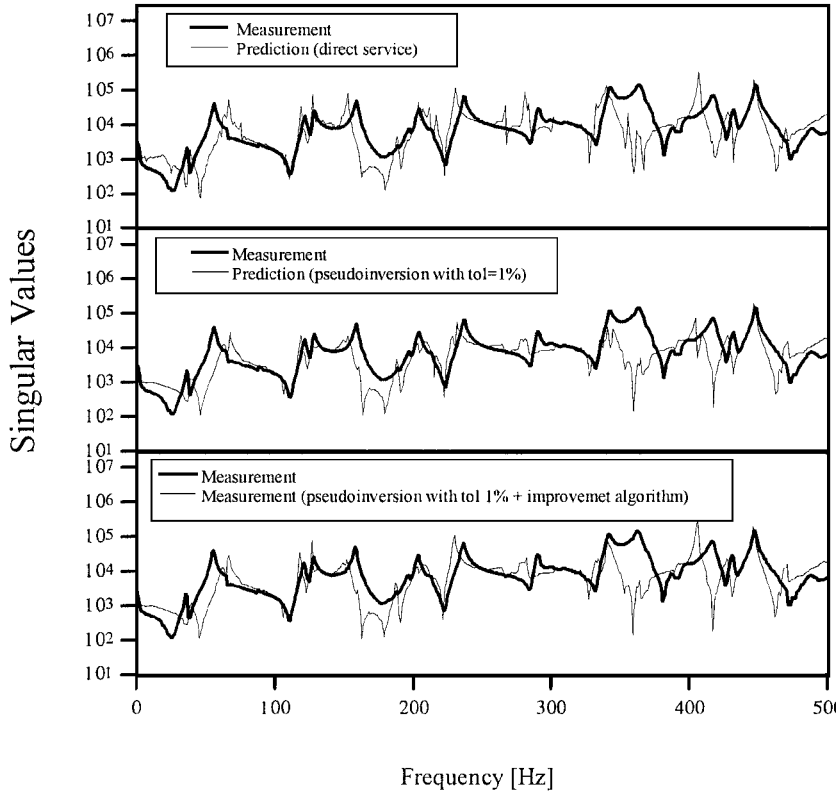

Fig. 6 Direct inversion vs pseudoinversion.

Table 1 Contributions to singular value 9

Frequency, Hz	Substructure *A*	Substructure *B*
403	−1.231*e*+4	1.528*e*+4
404	−1.140*e*+4	1.271*e*+4
405	1.168*e*+4	−1.115*e*+4
406	7.415*e*+3	−6.469*e*+3

Table 2 Contributions to singular value 6

Frequency, Hz	Substructure *A*	Substructure *B*
278	−9.833*e*+3	1.540*e*+4
279	1.3*e*+3	6.027*e*+3
280	4.878*e*+3	3.649*e*+3
281	6.348*e*+3	2.046*e*+3

and opposite (Table 1). Therefore, valuable structural information is omitted during the pseudoinversion.

B. Frequency Range 279–282 Hertz

In this frequency range, the four last singular values are neglected. In Tables 2–5, the values of the contributions of each substructure to each singular value are given. It can be observed that in this range almost all of the singular values have opposite contributions. The biggest participation to the chopping comes from the two last singular values.

C. Improvement Algorithm

From the analysis presented in the preceding section, it is clear that there is need for a methodology that will indicate if the singular values eliminated during the application of pseudoinversion must be taken into account. The steps of such an improvement algorithm are described as follows:

1) The rank of the matrix to be inverted is calculated using the same tolerance as the one that is used during the pseudoinversion. Then for each of the eliminated singular values the following steps are performed.

Table 3 Contributions to singular value 7

Frequency, Hz	Substructure *A*	Substructure *B*
278	253.1	3.9*e*+3
279	−684.6	6.539*e*+3
280	491	4.119*e*+3
281	2.038*e*+3	2.417*e*+3

Table 4 Contributions to singular value 8

Frequency, Hz	Substructure *A*	Substructure *B*
278	559.9	2.238*e*+3
279	−5.359*e*+3	6.898*e*+3
280	−2.336*e*+3	4.713*e*+3
281	4.579*e*+3	−2.923*e*+3

Table 5 Contributions to singular value 9

Frequency, Hz	Substructure *A*	Substructure *B*
278	−2.180*e*+3	4.034*e*+3
279	−1.833*e*+3	2.369*e*+3
280	−1.648*e*+3	2.2*e*+3
281	9.113*e*+3	−8.425*e*+3

2) The frequency lines where there are opposite contributions from the two substructures to the singular values are identified.

3) The absolute value of the negative contribution is taken, and successively the summation of the two contributions is calculated.

4) The result of this summation is compared with the larger singular value. If the outcome of the comparison is larger than 1% of the higher singular value (or generally speaking, larger than the tolerance that is used during the application of the pseudoinversion), then the singular value under examination is taken into account.

The results of this improvement algorithm are shown in the bottom part of Fig. 6. Obviously, the results preserve the most beneficial features of the pseudoinversion with TOL 1% (middle Fig. 6) and eliminate the majority of the inaccuracies (bottom Fig. 6). As far as the two representative cases are concerned, it can be seen that the chopping of the peak has been reduced (279–282 Hz) and that there is only one peak at the frequency range of 404–407 Hz.

VI. Conclusions

In this study, the problems encountered during the application of a coupling technique were investigated. The investigation shows that the lack of inclusion of the RDOF during the calculations results in the appearance of a negative frequency shift of the predictions. Furthermore, it was proven that another source of error is the direct inversion of a matrix that contains the FRFs of the substructures for the coupling points. Subsequently, the beneficial effect of the pseudoinversion by means of SVD on the prediction was demonstrated. Finally, some problems that were encountered due to the pseudoinversion were successfully dealt via a new improvement algorithm.

Acknowledgments

Part of this work was performed within the framework of the European Union BRITE/EURAM Project 7797: Vibroacoustic Modelling and Prediction of Transportation Vehicles Dynamic Behaviour in the Medium Frequency Range, as well as under the framework of the Human Capital and Mobiliy Project Method On Noise Identification Control Activities.

References

[1]Lammens, S., and Sas, P., "Modal Analysis and Testing," *Course on Modal Analysis Theory and Practice of 19th International Seminar on Modal Analysis Conference*, Katholieke Universiteit Leuven, Leuven, Belgium, 1994.

[2]Spyrakos, C., "Finite Element Modeling in Engineering Practice," Univ. Press, West Virginia, 1994.

[3]Imregun, M., Rodd, D. A., and Ewins, D. J., "Structural Modification and Coupling Dynamic Analysis Using Measured Frequency Response Function (FRF) Data," *Proceedings of the 5th International Madal Analysis Conference*, Society of the Experimental Mechanic, Bethel, CT USA, 1987, pp. 1136–1141.

[4]Ewins, D. J., "Modal Analysis at High Frequencies," *Proceedings of the International Symposium: Prediction of the Noise Emitted by Vibrating Structures*, Centre for Technology and Innovation Management-Senlis, France, 1991, pp. 175–191.

[5]Duarte, M. L. M., and Ewins, D. J., "Some Insights into the Importance of Rotational Degrees-of-Freedom and Residual Terms in Coupled Structure Analysis," *Proceedings of the 13th International Modal Analysis Conference*, Society of the Experimental Mechanic, Bethel, CT, 1995, pp. 164–170.

[6]Van Loon, P., "Modal Parameters of Mechanical Structures," Ph.D. Dissertation, Dept. of Mechanical Engineering, Katholieke Universiteit Leuven, Leuven, Belgium, 1974.

[7]Brandon, J., "On Numerical Analysis Needs for Modal Analysis," *Proceedings of 7th International Modal Analysis Conference*, Vol. 1, Society of the Experimental Mechanic, Bethel, CT, 1989, pp. 331–334.

[8]Liang, Z., and Inman, D. J., "A Tutorial on Matrix Inversion in Time Domain Modal Analysis," *Proceedings of the 7th International Modal Analysis Conference*, Vol. 1, Society of the Experimental Mechanic, Bethel, CT, 1989, pp. 324–330.

[9]Ibrahim, S. R., "The Condition of Matrix Inversion in Modal Analysis," *Proceedings of the 7th International Modal Analysis Conference*, Vol. 1, Society of the Experimental Mechanic, Bethel, CT, 1989, pp. 307–312.

[10]Bregant, L., Otte, D., and Sas, P., "FRF (Frequency Response Function) Substructure Synthesis: Evaluation and Validation of Data Reduction Methods," *Proceedings of the 13th International Modal Analysis Conference*, Society of the Experimental Mechanic, Bethel, CT, 1995, pp. 1592–1597.

[11]Gialamas, T., Tsahalis, D., Bregant, L., Otte, D., and Van der Auweraer, H., "Substructuring by Means of FRFs (Frequency Response Functions): Some Investigations on the Significance of Rotational DOFs (Degrees of Freedom)," *Proceedings of the 14th International Modal Analysis Conference*, Society of the Experimental Mechanic, Bethel, CT, 1996, pp. 619–625.

[12]Maix, N. M. M., "An Introduction to the Singular Value Decomposition Technique (SVD)," *Proceedings of the 7th International Modal Analysis Conference*, Society of the Experimental Mechanic, Bethel, CT, 1989, pp. 335–339.